



American Journal of *Energy*
and *Power Engineering*

Keywords

Free and Forced Convection,
Rectangular Box,
Parallel Heated Plates,
Vertical and Horizontal Heaters

Received: January 20, 2015

Revised: January 30, 2015

Accepted: January 31, 2015

Free and Forced Convection Heat Transfer Characteristics in an Opened Box with Parallel Heated Plates

Laith Jaafer Habeeb, Wahid Shati Mohammad,
Maher Abdalrazaq Rashed

University of Technology, Mechanical Engineering Department, Baghdad, Iraq

Email address

laithhabeeb1974@gmail.com (L. J. Habeeb), wahid_1953@yahoo.com (W. S. Mohammad),
every1989@yahoo.com (M. A. Rashed)

Citation

Laith Jaafer Habeeb, Wahid Shati Mohammad, Maher Abdalrazaq Rashed. Free and Forced Convection Heat Transfer Characteristics in an Opened Box with Parallel Heated Plates. *American Journal of Energy and Power Engineering*. Vol. 2, No. 1, 2015, pp. 1-11.

Abstract

This paper represents an experimental investigation of forced and free convection heat transfer for three dimension laminar steady flows in three-dimensional space as rectangular box. The experiments include a study of the effect of forced and free convection heat transfer and the effect of the position of the two parallel heated plates in an enclosure. This experimental work includes two cases: First case: represents the study of heat transfer characteristics by forced convection for the exit air from the top circular hole for Reynolds number range at all power range. The results show that the average Nusselt number increases with increase of the power. Second case: represents the study of heat transfer characteristics by free convection for the entry of the air from the circular hole on the bottom face of the box and the exit air is from the circular one hole or two holes of the top face of the box for an average Nusselt number range (mode-a) in the case of one hole for the exit air from the top, and for an average Nusselt number range (mode-b) in the case of two holes for the exit air from the top. The experimental results show that the average Nusselt number inversely proportional with Rayleigh number for high heater power values. The average Nusselt number increases with the increase of Reynolds number for the first case.

1. Introduction

The satisfactory performance of electronic equipment depends on their operating temperature. In order to maintain these devices within the safe temperature limits, an effective cooling is needed. High heat transfer rate, compact in size and reliable operation are the challenges of a thermal design engineer of electronic equipment. Air cooling is suitable for low heat dissipating devices. Natural convection and forced convection are the two types of air cooling used. Calcagni et al. 2005, studied the heat transfer in square enclosures heated from below. The paper deals with the results of an experimental and numerical study of free convective heat transfer in a square enclosure characterized by a discrete heater located on the lower wall and cooled from the lateral walls. The study analyzed how the heat transfer develops inside the cavity at the increasing of the heat source length. The local Nusselt number was evaluated on the heat source surface and it shows a symmetrical form raising near the heat source borders. Nada 2007, investigated the Natural convection heat transfer in horizontal and vertical

closed narrow enclosures with heated rectangular finned base plate. In comparison with enclosure of a bare base plate, insertion of heat conducting fins always enhances heat transfer rate. Useful design guidelines have been suggested. Correlations of Nu_H have been developed for horizontal and vertical enclosures. Nader et al. 2007, studied the thermal boundary conditions on natural convection in a square enclosure partially heated from below. Natural convection in air-filled 2D square enclosure heated with a constant source from below and cooled from above was studied numerically for a variety of thermal boundary conditions at the top and sidewalls. Simulations were performed for two kinds of lengths of the heated source, i.e., a small and a large source corresponding to 20% and 80% of the total length of the bottom wall, respectively. Comparisons among the different thermal configurations considered were reported. Sattar 2007, Investigated the heat transfer phenomena and flow behavior around electronic chip. Computational study of three-dimensional laminar and turbulent flows around electronic chip (heat source) located on a printed circuit board were presented. Computational field involves the solution of elliptic partial differential equations for conservation of mass, momentum, energy, turbulent energy, and its dissipation rate in finite volume form. The chip was cooled by an external flow of air. The results show the relation between the temperature rise, heat transfer parameters (Nu , Ra) with [Archimedes Number(Ar), Heat Dissipation(Q)] for two cases of laminar and turbulent flows. Mustapha and Hamid 2010, investigated numerically the free convection dominated melting in an isolated cavity heated by three protruding electronic components. The heat sources generate heat at a constant and uniform volumetric rate. The advantage of using this cooling strategy was that the PCMs were able to absorb a high amount of heat generated by electronic components without activating the fan. A parametric study was conducted in order to optimize the thermal performance of the heat sink. The optimization involves determination of the key parameter values that maximize the time required by the electronic component to reach the critical temperature ($T < T_{cr}$). Geniy and Mikhail 2011, studied the natural convection in an enclosure with a heat source of constant heat transfer rate. The natural convection in a rectangular enclosure having finite thickness heat-conducting walls with a heat source of constant heat transfer rate located on the inner side of the left wall in conditions of convection–radiation heat exchange with an environment on one of the external boundaries has been performed. Deka 2006, studied the skin-friction for unsteady free convection flow between two heated vertical parallel plates. Unsteady viscous incompressible free convection flow of an electrically conducting fluid between two heated vertical parallel plates was considered in the presence of a uniform magnetic field applied transversely to the flow. The induce field along the lines of motion varies transversely to the flow and the fluid temperature changing

with time. It has been observed that with the increase in Rm , the magnetic Reynolds number, at constant M , the Hartmann number, leads to an increase in the skin-friction gradually. But with the increase in M , at constant Rm , the skin-friction decreases. Fahad and Maged 2012, studied the mixed convection with surface radiation between two asymmetrically heated vertical parallel plates. The effect of surface radiation on the developing laminar mixed-convection flow of a transparent gas between two asymmetrically heated vertical parallel plates was investigated. The effect of surface radiation on wall temperatures, fluid temperature profiles, location of the channel height at which the buoyancy forces balance the viscous forces, the location of the onset of pressure build up, the location of the onset of flow reversal, average friction factor, and Nusselt number were illustrated. The values of the emissivity at which surface radiation engenders minimum pumping power requirements were obtained. Han-Taw, Chung-Hou, Tzu-Hsiang and Ge-Jang 2014, applied the inverse method and three-dimensional CFD commercial software in conjunction with the experimental temperature data to investigate the heat transfer and fluid flow characteristics of the plate-fin heat sink in a closed rectangular enclosure for various values of fin height. The inverse method with the finite difference method and the experimental temperature data was applied to determine the heat transfer coefficient. The $k-\epsilon$ turbulence model was used to obtain the heat transfer and fluid flow characteristics within the fins. To validate the accuracy of the results obtained, the comparison of the average heat transfer coefficient was made. The aim of the present work is to study experimentally a three-dimensional free and forced convection heat transfer characteristics in an enclosure containing parallel heated plates arranged horizontally and vertically inside the enclosure relative to the direction of the air stream to maximize heat transfer with different velocities and powers. Also to study the effect of changing the location of exit regions in different cases on average Nusselt number values, so to help manufacturers where to put the holes on the electronic devices containers.

2. Experimental Apparatus and Data Reduction

2.1. Test Rig Description

The test rig is designed and manufactured to fulfill the requirements of the test system for forced convection heat transfer. The experimental apparatus consists basically of the test section, electrical heater and voltage regulator, air fan with velocity regulator, selector switch, and the measuring devices. Most of these parts are manufactured, and care was taken to prevent any air leakage between the connected sections during operation and re-fixing. Figure (1) shows the photograph of the test rig, and figure (2) illustrates the schematic diagram of the experimental apparatus.

2.2. The Test Section

The experimental model used in the present study is a box and plate heaters, the main dimensions of the box are; length ($L=45$ cm), width ($W=30$ cm) and height ($H=40$ cm), as shown in Figure (3-a&b). All the walls of the box are constructed from a plastic glass of thickness (4 mm). In the center of the box there are two parallel plate heaters fixed to the wall of the box. The distance between the heaters is (10 cm) as shown in Figure (3-a) for the two cases for forced and free convection. Case (1): forced convection for the parallel plates and the outlet air is from the top hole only. Case (2): free convection for two modes (mode-a: inlet air from the bottom and one outlet air from the top) and (mode-b: inlet air from the bottom and two outlet air from the top). The partially opened opposite sides of the box are punctured with three circular holes of diameter (10 cm). The first hole is for air inlet and the other two holes are for air outlet. One hole is drilled in the upper wall for entry of (19) thermocouples measure the temperatures inside the box. The temperature is monitored with thermocouples. The thermocouples are arranged to form a tree in order to measure the temperature at different locations according to the grid distribution. The grids are distributed horizontally and vertically in order to take into accounts all the temperature variation in the model, as shown in Figure (4).

3. Layout and Measured Parameters

During the experimental investigation, the main parameters measured are:-

1. The temperature of air entering and leaving the test section.
2. The surface temperature of the box.
3. The temperature distribution within the test section.
4. The velocity of air entering and leaving the test section.
5. The voltages and currents supplied to the heaters.

Experiments are carried out to study the effect of Reynolds number, power, and heat source arrangement for forced convection inside the enclosure, in addition to two exit zone locations.

4. Experimental Procedures

Experiments were conducted to measure the velocities, temperatures and power. The experimental work is done in a specially designed box with thermocouples distributed in three dimensions. The general steps followed in this experimental investigation for forced convection, are given:

4.1. Forced Convection

1. The power is turn on to the fan and the air velocity is adjusted to the test section using the voltage regulator to the first air velocity required (1.5) m/s and setting the accessories to the other selected specifications.
2. The readings of all thermocouples are recorded from the

selector switch before supplying the power to the heaters.

3. Electrical power is then supplied to the heaters to calculate the required outlet power from the heaters by adjusting the voltage regulator in accordance to the required first power. The power is measured by using the voltage and current measuring devices.
4. After about (30-100) minutes the steady-state condition is reached, then recording the temperatures distribution through the box using the 19 thermocouples.
5. Steps (1-4) are repeated for the other two air velocities (2.6, 3.5) m/s for the same heaters power.
6. The electrical power supply is turned off and the rig is left to cool for a sufficient time, so the temperature distribution becomes uniform and equal to the room temperature.
7. The steps (1-6) are then repeated for the other two power.

4.2. Free Convection

1. The readings of all thermocouples are recorded from the selector switch before supplying the power to the heaters.
2. Electrical power is supplied to the heaters to calculate the required outlet power from the heaters by adjusting the voltage regulator in accordance to the first heat flux required. The power is measured by using the voltage and current measuring devices.
3. About (30-100) minutes of waiting till to reach the steady-state condition. Then the temperatures distribution is recorded through the box using the 19 thermocouples.
4. Electrical power supply is then switched off and the rig left for a sufficient time to cool, so the temperature distribution becomes uniform and equal to the room temperature.
5. Steps (1-4) are repeated for the other three powers for the two modes; mode-a: inlet air enters from the bottom circular hole and outlet air leaves from one top circular hole, and mode-b: inlet air enters from the bottom hole and outlet air leaves from two top holes.

5. Basic Equations of Calculations

5.1. Air Velocity

The inlet velocity is used to define the flow velocity through the test section. For laminar flow in the box, the velocity is computed from air flow rate at box inlet, the air velocity through the box can be determined by:

For assumption: $Q_1 = Q_2$

$$V_1 A_1 = V_2 A_2 \quad (1)$$

There are three values of the inlet velocity at the test section (box) have been selected in the present work, which are (0.098125, 0.17008, 0.2028) m/s.

5.2. Heat Transfer Coefficient

The average heat transfer coefficient (for free convection and forced convection) can be calculated by:

$$h_{av} = \frac{P_t}{A(t_s - t_{air})} \quad (2)$$

5.3. Nusselt Number

The average Nusselt number (Nu_{av}) can be determined by:-

$$Nu_{av} = \frac{h_{av} D_h}{K} \quad (3)$$

5.4. Reynolds Number

For the forced convection case, the average Reynolds number based on the hydraulic diameter and the actual velocity within the box can be determined by: -

$$Re = \frac{\rho \times V_2 \times D_h}{\mu} \quad (4)$$

5.5. Rayleigh Number

The Rayleigh number can be determining by:

$$Ra = \frac{g \beta (T_s - T_{air}) L^3}{\nu} Pr \quad (5)$$

Where:

$g = 9.81 \text{ m}^2/\text{s}$, $\beta = 6.39965 \times 10^{-3} \text{ k}^{-1}$ (measured), $L = 0.3 \text{ m}$, $\nu = 2.86 \times 10^{-5} \text{ m}^2/\text{s}$ (from tables), $pr = 0.70275$ (from tables), $T_s = 259.65 \text{ }^\circ\text{C}$ (measured), $T_{air} = 52.867 \text{ }^\circ\text{C}$ (measured)

6. Error Analysis

The uncertainties in the heat transfer coefficient is presented in uncertainties in the average Nusselt number, which depends upon the uncertainties in, which depends upon the uncertainties in:

- The temperature difference between the entering air temperature and leaving air temperature at the test section (ΔT_a).
- The temperature difference between the average surface temperature of the heated plates and average air temperature at the test section (ΔT_s).
- Air velocity.

A final reasonable value corresponds to the Pythagorean summation of the discrete uncertainties, i.e.

$$U_f = \left[\sum_{i=1}^n \left\{ \left(\frac{\partial f}{\partial x_i} \right) U_{x_i} \right\}^2 \right]^{0.5} \quad (6)$$

Where

x_i = Nominal values of variables.

U_{x_i} = Discrete uncertainties associated with x_i variable.

U_f = Overall uncertainty associated with function.

The uncertainties in each individual measurement lead to uncertainties of the experiment, which are given in table (1).

Table (1). The uncertainties in each individual measurement

Measure Parameter	Uncertainties
Air temperature	$\pm (0 \text{ to } 0.5) \text{ }^\circ\text{C}$
Air velocity	$\pm 2 \%$
Average Nusselt number	8.226 %

7. Results and Discussion

The temperature will affect the fluid flow in the internal flow and will complicate the assumptions of heat transfer, particularly laminar flow at low Reynolds number. The effect of the buoyancy can't be neglected.

7.1. Temperature Distributions of the First Case

Figures (5) to (8) illustrate the temperature variation plots inside the test section for case (1). It show that the readings obtained by thermocouples inside the box at different planes in three dimensions for various powers and air velocities. The recorded readings shown in these figures were taken for many planes (in X, Y & Z-directions) to exhibit the thermal gradient and the effect of power and air velocity. It can be seen that for a given power and air velocity, the temperature in the box progressively decreases away from hot plates. This indicates that the temperature distribution pattern becomes more linear owing to the vigorous convective flow and the thermal boundary layer influence becomes small at these locations.

7.2. Nusselt and Reynolds Numbers of Case (1)

The variation of the local Nusselt number (Nu) with the X-axis was plotted in figures (9) to (12). The local Nusselt number increases with the X-axis along the flow direction to the middle of the box and then the local Nusselt number value decreases. The local Nusselt number will then decrease with the X-axis along the flow direction for ($V=3.1 \text{ m/s}$) at ($P_f=316.35 \text{ W}$) as shown in figure (10).

The rate of increase of average Nusselt number is begins to increase with the increase of air velocity until ($V=2.6 \text{ m/s}$) and then the average Nusselt number value decreases as shown in figure (12). This may be attributed to the location of the outlet circular hole which is relatively upper than the inlet one which make a lot of circulation before the air exiting from the box and the high momentum dose not exit directly from the box and take a long time inside, hence increase the temperature instead of decrease it.

7.3. Temperature Field of the Second Case

The steady state temperature distributions along the box (X, Y and Z) direction are illustrated in figures (13) to (16). Figures (13, 14) show the temperatures distribution inside the box in the case of free convection for inlet air vent from the bottom and one outlet air vent from the top (mode-a). Figures (15, 16) show the temperatures distribution inside the box in the case of free convection for inlet air vent from the bottom and two outlet air vents from the top (mode-b).

7.4. Nusselt and Rayleigh Numbers of Case (2)

Heat transfer rates in terms of Nusselt number are presented in figures (17 & 18) for (mode-a) and (mode-b) respectively. As seen from this figure the average Nusselt number increases with Rayleigh number decrease along the flow direction. The rate of free convection heat transfer is inversely proportional with Rayleigh number for high heater power values. This is due to inefficient natural convection with these large values of power input, then it is required a more convenient device to help removing the heat.

8. Correlations Equations

In order to describe the relationship between the dependent variable (Nusselt number) and the independent variables (Rayleigh number, Reynolds number), a correlation was made based on the following simplified version:

The average Nusselt number (Nu_{av}) value plotted as a function of Reynolds Number (Re) for each power (P_i).

Then from figure (12) for case (1):

$$Nu_{av} = 86.77 Re^{0.1399} \quad \text{for (power=418.08 W)}$$

$$Nu_{av} = 81.399 Re^{0.1054} \quad \text{for (power=316.35 W)}$$

$$Nu_{av} = 34.303 Re^{0.2161} \quad \text{for (power=211.87 W)}$$

The average Nusselt number (Nu_{av}) value plotted as a function of Rayleigh number (Ra) for each power (P_i). Then From figure (17) and (18) for case (2), the correlations equations are:-

$$Nu_{av} = 468120 Ra^{0.418} \quad \text{for mode-a}$$

$$Nu_{av} = 5.6906 Ra^{0.19} \quad \text{for mode-b}$$

9. Conclusions

The following points can be concluded from the present experimental work:

1. The natural convection is inefficient to cool box for all the power input when tested for case (2) (mode-a and mode-b). Therefore the forced convection mode is required.
2. The maximum temperature is noticed to be in between

the heaters for both horizontal and vertical conditions and for the two cases. Therefore it is required a good location when choosing the fan location and the configuration of its exit.

3. The rate of free convection heat transfer case (2) is inversely proportional with Rayleigh number for high heater power values. This is due to inefficient natural convection with these large values of power input, then it is required a more convenient device to help removing the heat.
4. In case (1) the average Nusselt number is begins to increase with the increase of air velocity until ($V=2.6$ m/s) and then the average Nusselt number value decreases.
5. The results of the two cases show that the best case of heat transfer occurs when the heat is transferred by forced convection (case (1)).
6. The advantage of free convection is there is no additional power for fans, where the disadvantage is it is not efficient to cool high power circuits. While the advantage of forced convection is it is used in the most applications and the disadvantage is it uses additional electrical power and cost.



Figure (1). Photograph of the test rig.

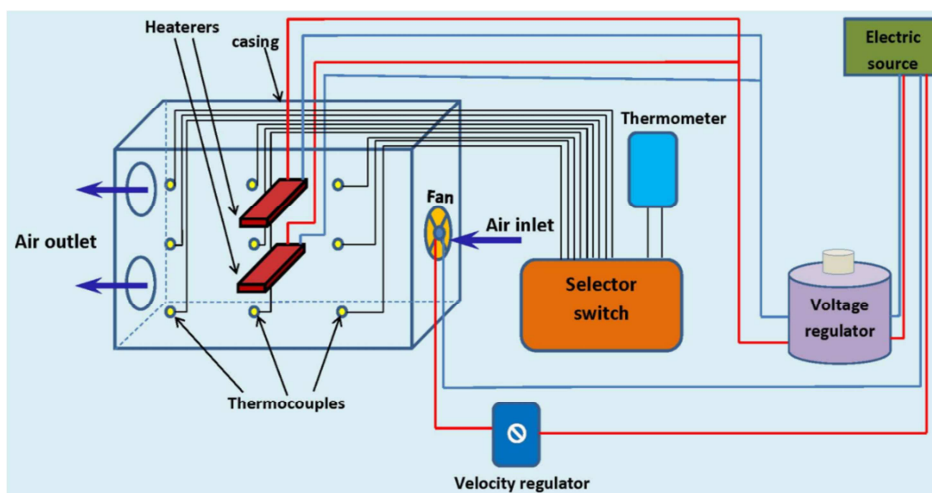


Figure (2). Schematic diagram of the experimental apparatus.

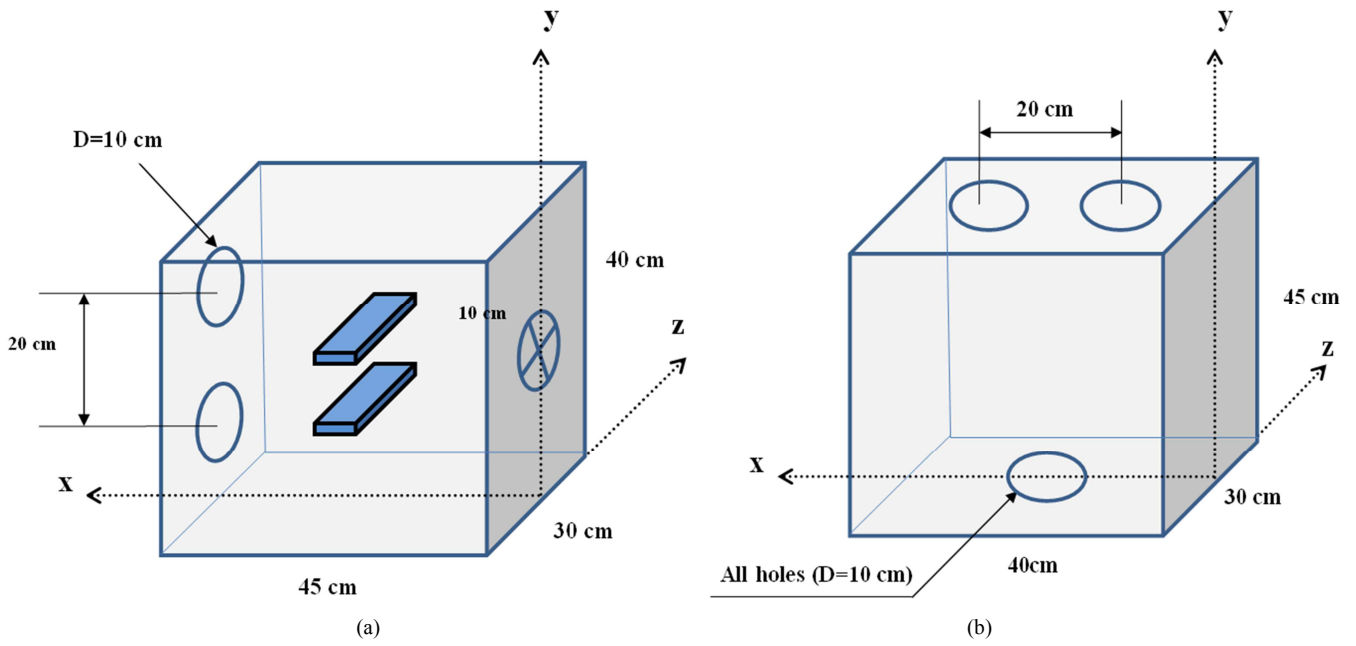


Figure (3). (a) box description for the first case. (b) box description for the second case.



Figure (4). Thermocouples distribution on grid inside test section.

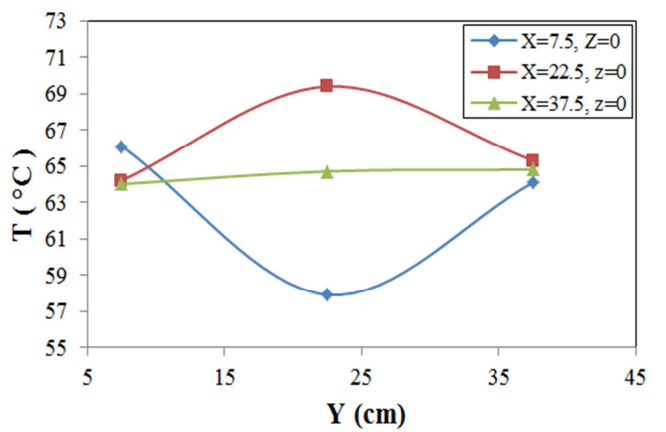
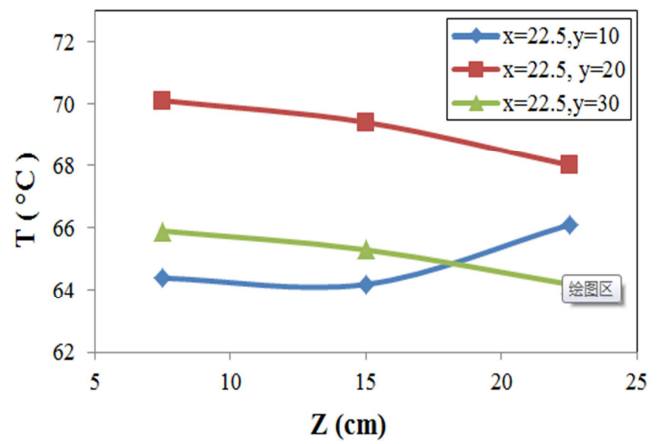
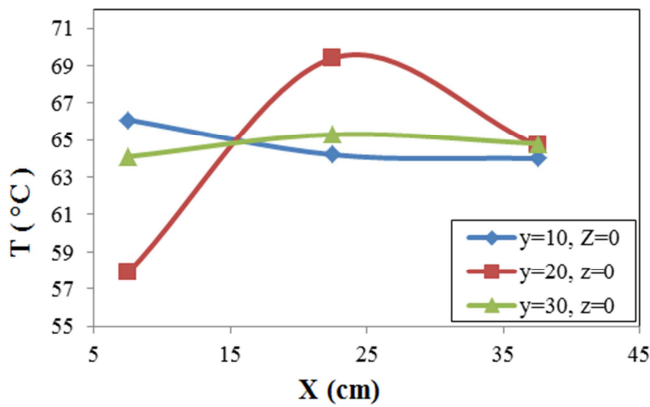


Figure (5). Temperature distribution for forced convection case (1) at $V=2.6$ m/s, $P_t=418.08$ W



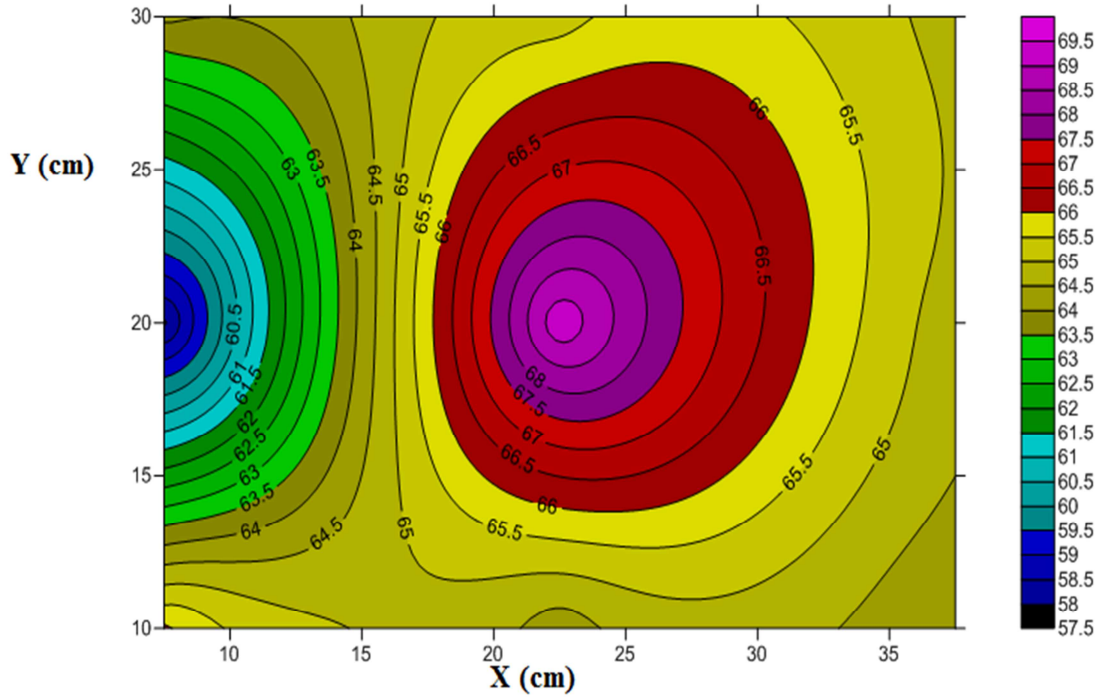


Figure (6). Temperature contours for forced convection case (1) at $V=2.6$ m/s, $P_t=418.08$ W

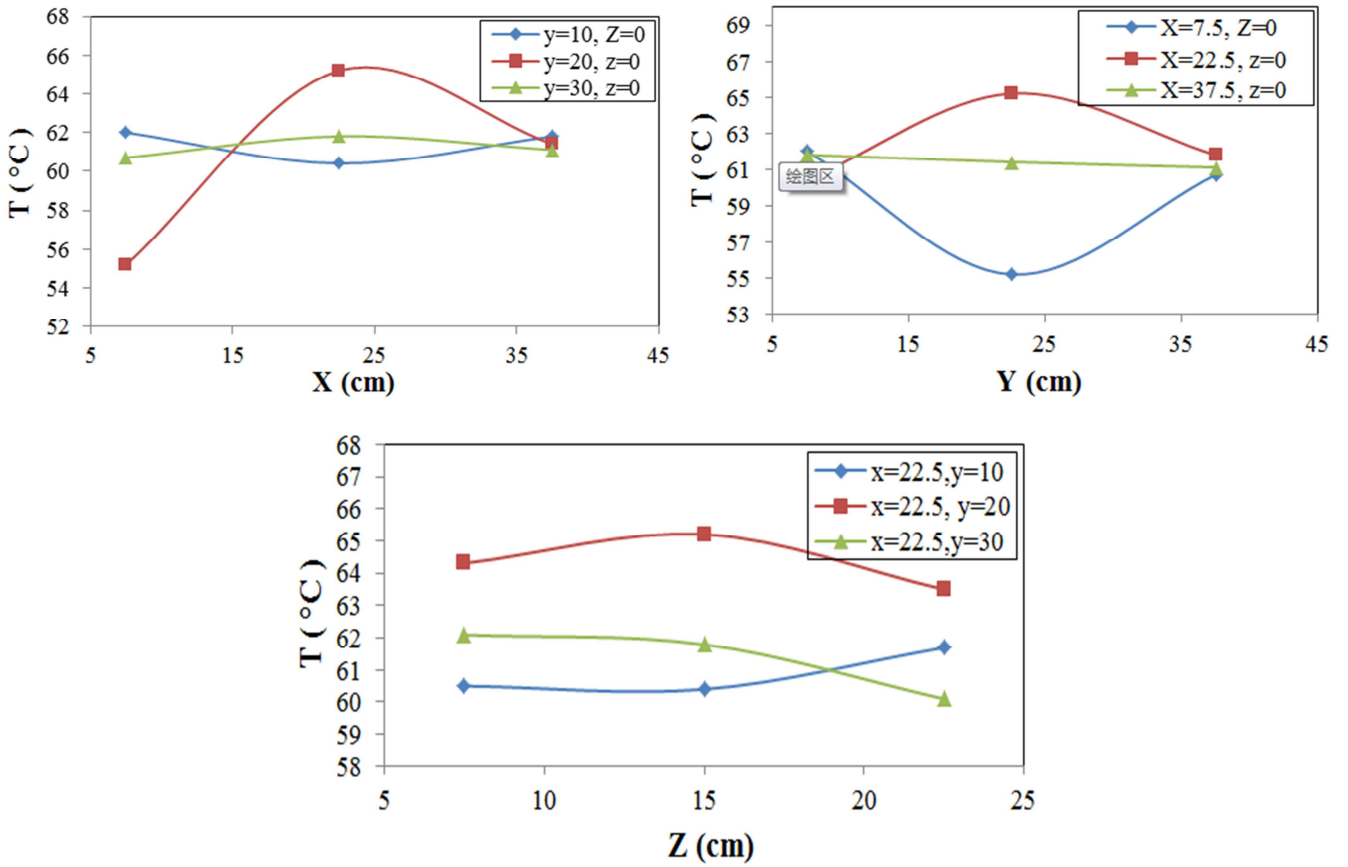


Figure (7). Temperature distribution for forced convection case (1) at $V=2.6$ m/s, $P_t=316.35$ W

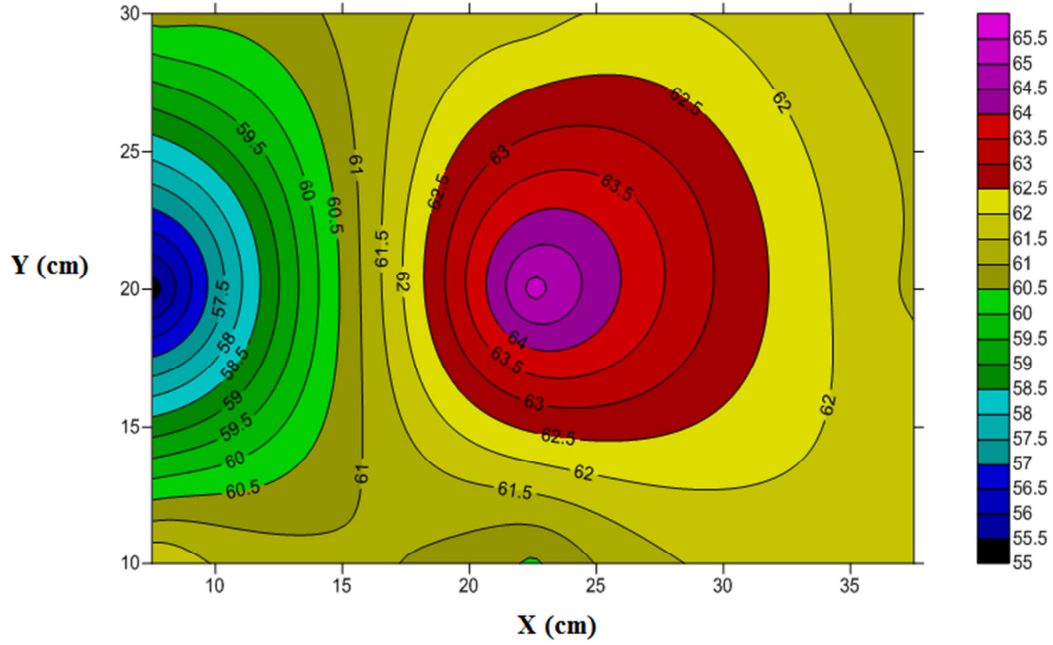


Figure (8). Temperature contours for force convection case (1) at $V=2.6$ m/s, $P_i=316.35$ W

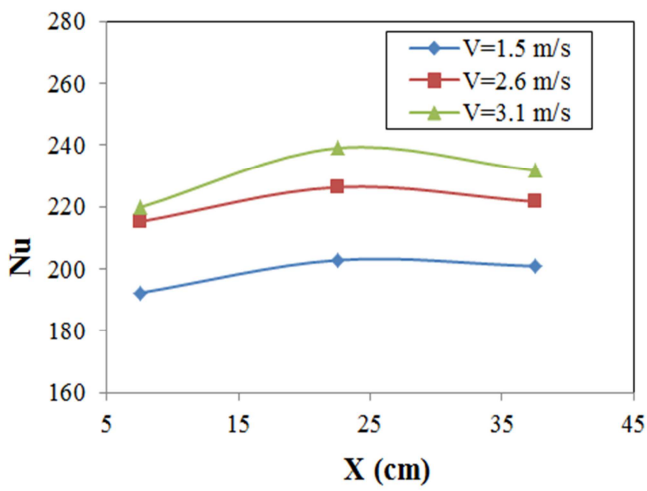


Figure (9). Variation of local Nusselt number with X-axis for forced convection case (1) at $P_i=418.08$ W

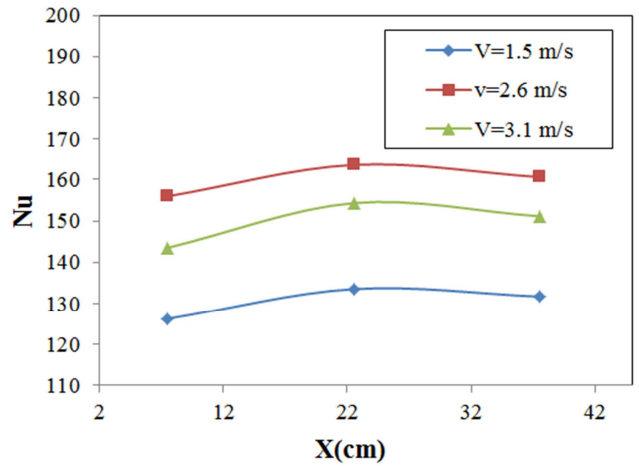


Figure (11). Variation of local Nusselt number with X-axis for forced convection case (3) at $P_i=211.87$ W

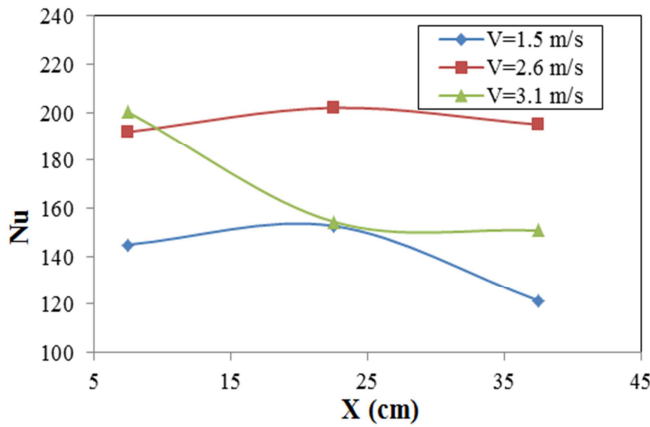


Figure (10). Variation of local Nusselt number with X-axis for forced convection case (3) at $P_i=316.35$ W

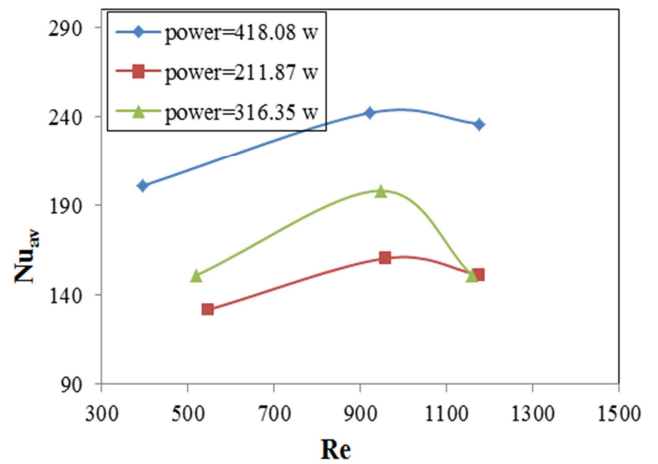


Figure (12). Variation of average Nusselt number with Reynolds number for forced convection for case (3).

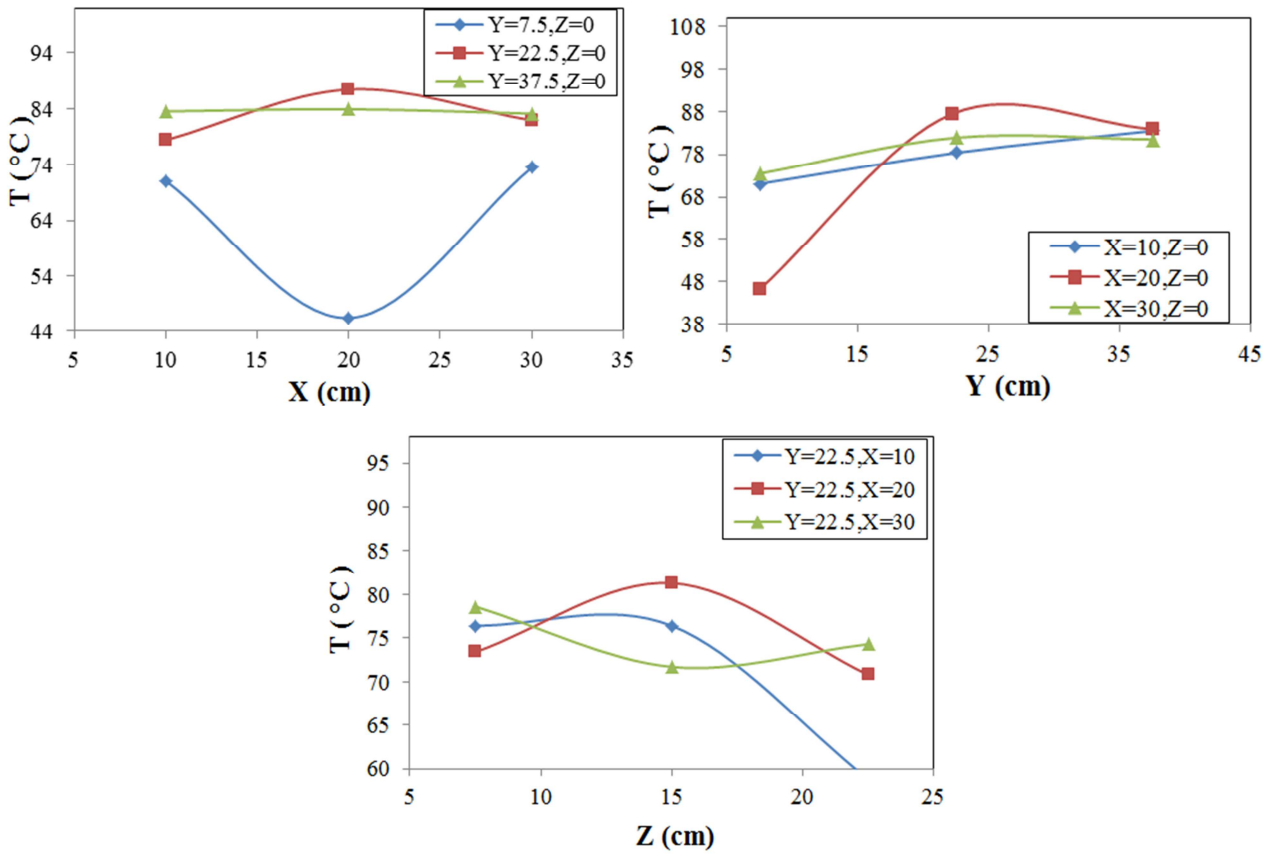


Figure (13). Temperature distribution for free convection (mode-a) at ($P_i = 211.87$ W).

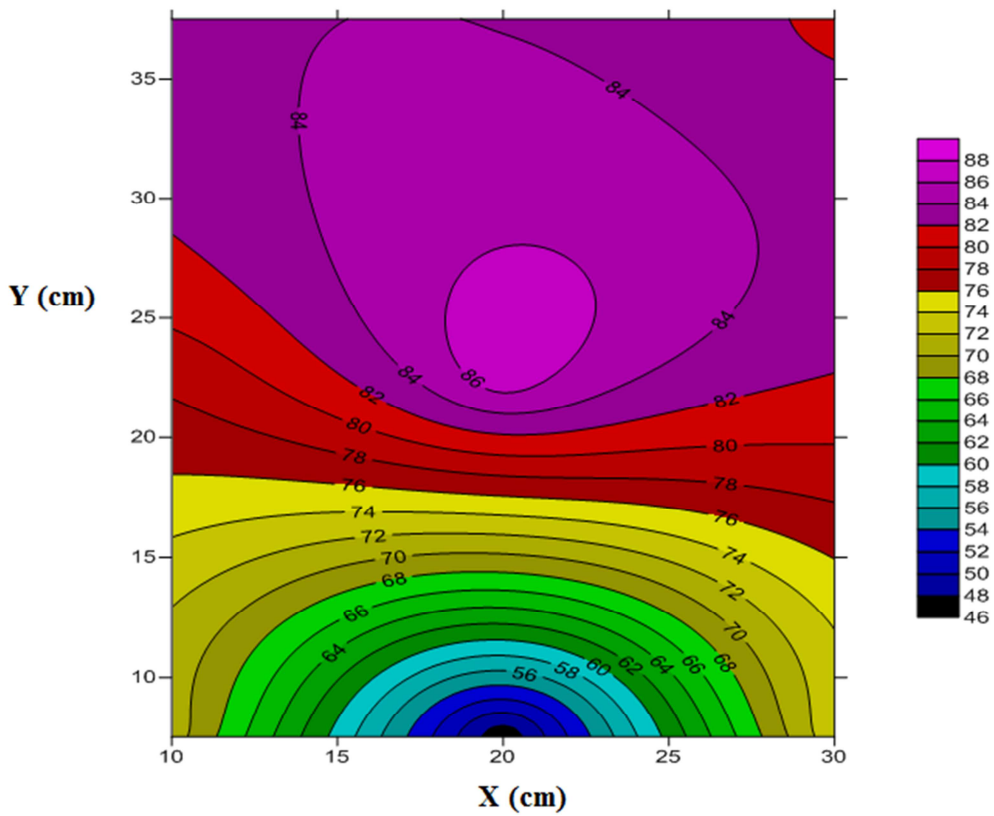


Figure (14). Temperature contours for free convection (mode-a) at ($P_i = 211.87$ W)

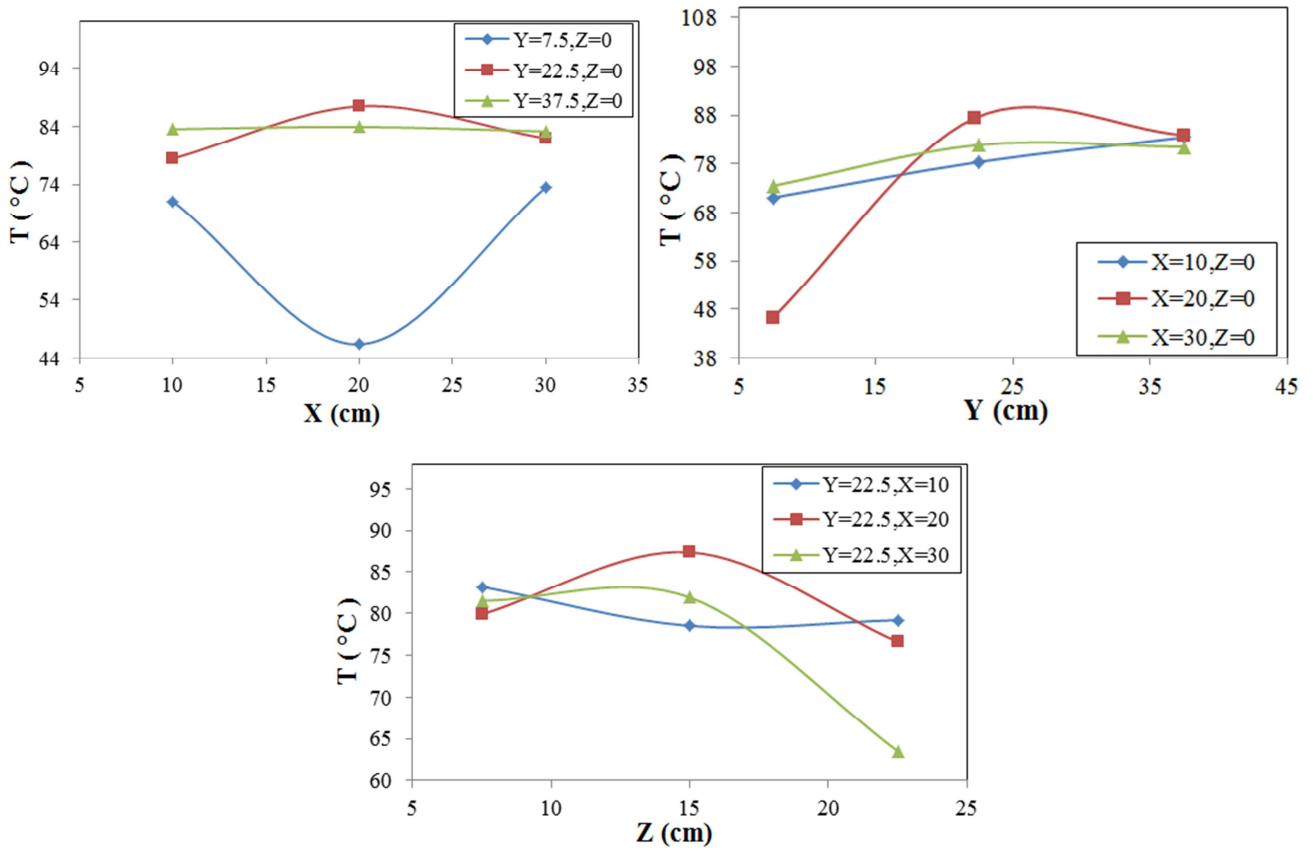


Figure (15). Temperature distribution for free convection (mode-b) at $(P_i = 211.87 \text{ W})$.

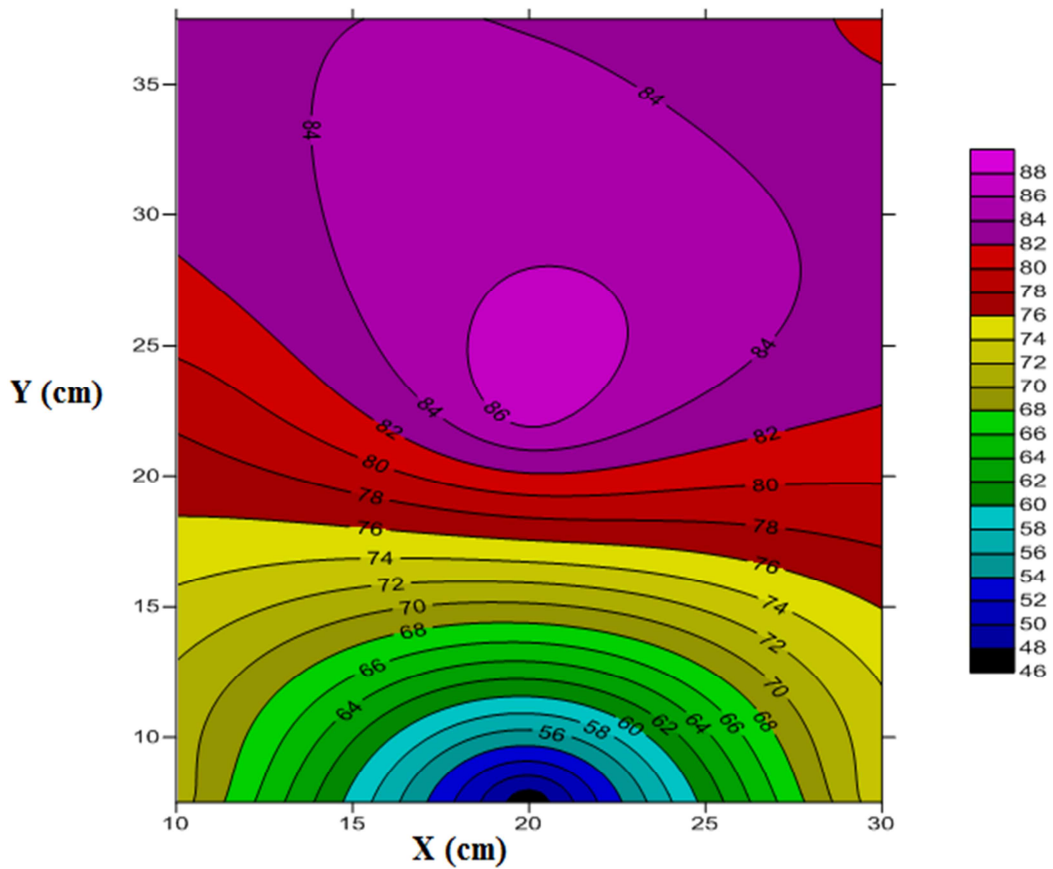


Figure (16). Temperature contours for free convection mode-b at $(P_i = 211.87 \text{ W})$

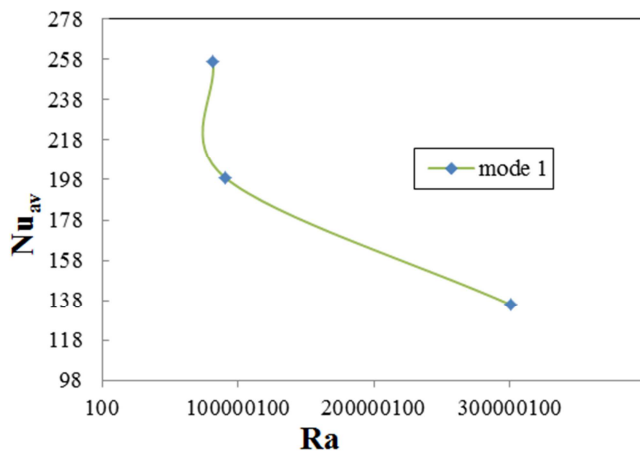


Figure (17). Variation of the average Nusselt number with Rayleigh number for free convection (mode-a) at $P_t = (96.63, 211.87 \text{ and } 316.35) \text{ W}$

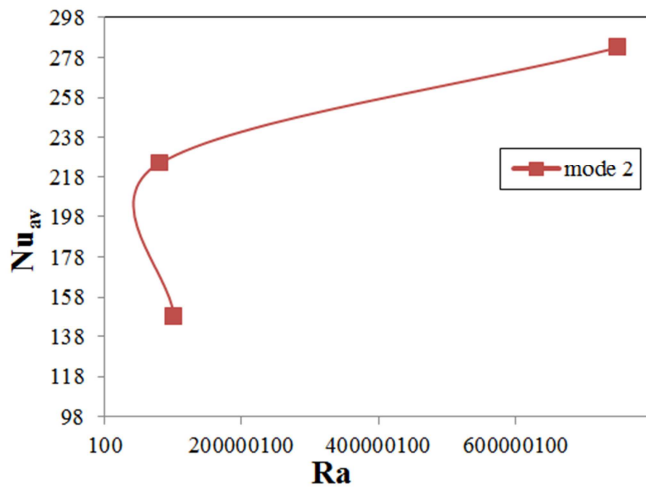


Figure (18). Variation of the average Nusselt number with Rayleigh number for free convection (mode-b) at $P_t = (96.63, 211.87 \text{ and } 316.35) \text{ W}$

Nomenclature

A	Cross section area of heater surface.	m^2
$A1$	Cross sectional area of the circular hole.	m^2
$A2$	Cross sectional area through the box.	m^2
V	Fan air velocity.	m/s
$V1$	Air velocity at inlet of the test section (box).	m/s
$V2$	Air velocity through the box.	m/s
h_{av}	average heat transfer coefficient.	$\text{W/m}^2 \cdot \text{C}^\circ$
P_t	total power for heaters.	W
T_s	Surface temperature of the heater.	C°
T_{air}	Average temperature of the air.	C°

K	thermal conductivity of the air.	$\text{W/m} \cdot \text{C}^\circ$
D_h	Hydraulic diameter.	m
ρ	Density of the air.	Kg/m^3
μ	Dynamic viscosity of the fluid.	$\text{Kg/m} \cdot \text{s}$
K	Thermal conductivity.	$\text{W/m} \cdot \text{C}^\circ$
L	Characteristic length.	m
g	Acceleration due to gravity.	m^2/s
β	Thermal coefficient of volume expansion.	K^{-1}
ν	kinematic viscosity of the fluid.	m^2/s

References

- [1] B. Calcagni, F. Marsili and M. Paroncini, 2005. Natural Convective Heat Transfer in Square Enclosures Heated from Below, Applied Thermal Engineering 25, pp.2522-2531.
- [2] Fahad G. Al-Amri and Maged A.I. El-Shaarawi, 2012. Mixed Convection with Surface Radiation between Two Asymmetrically Heated Vertical Parallel Plates, International Journal of Thermal Sciences 58, pp.77-78.
- [3] Geniy V. Kuznetsov and Mikhail A. Sheremet, 2011. Conjugate Natural Convection in an Enclosure with a Heat Source of Constant Heat Transfer Rate, International Journal of Heat and Mass Transfer 54, pp.260-268.
- [4] Han-Taw Chen, Chung-Hou Lai, Tzu-Hsiang Lin and Ge-Jang He (2014). Estimation of Natural Convection Heat Transfer from Plate-Fin Heat Sinks in a Closed Enclosure. International Journal of Mechanical, Aerospace, Industrial and Mechatronics Engineering, Vol:8 No:8.
- [5] Mustapha Faraji and Hamid El Qarnia, 2010. Numerical Study of Free Convection Dominated Melting in an Isolated Cavity Heated by Three Protruding Electronic Components, IEEE transactions on components and packaging technologies, vol. 33, no. 1.
- [6] Nader Ben Cheikh, Brahim Ben Beya and Taieb Lili, 2007. Influence of Thermal Boundary Conditions on Natural Convection in a Square Enclosure Partially Heated from Below, International Communications in Heat and Mass Transfer 34, pp.369-379.
- [7] P. N. Deka, 2006. Skin-Friction for Unsteady Free Convection MHD flow between Two Heated Vertical Parallel Plates, Appl. Mech., Vol.33, No.4, pp. 259-280, Belgrade.
- [8] S. A. Nada, 2007. Natural Convection Heat Transfer in Horizontal and Vertical Closed Narrow Enclosures with Heated Rectangular Finned Base Plate, International Journal of Heat and Mass Transfer 50, pp.667-679.
- [9] Sattar J. Habeeb, 2007. Investigation of Heat Transfer Phenomena and Flow Behavior around Electronic Chip, Al-khwarizmi engineering journal, vol.3, no. 2, pp.17-31.